Electronic States and Potential Energy Curves of Zirconium and Hafnium Carbon Monoxide

Hang Tan,[†] Muzhen Liao,[‡] and K. Balasubramanian*,[†]

Department of Chemistry and Biochemistry, Arizona State University, Tempe, Arizona 85287-1604, and Department of Chemistry, Tsinghua University, Beijing 100084, China

Received: September 3, 1997; In Final Form: October 1, 1997

The potential energy surfaces for the low-lying electronic states of the zirconium carbon monoxide (ZrCO) and hafnium carbon monoxide (HfCO) systems have been studied using the complete active space multiconfiguration self-consistent field followed by multireference singles + doubles configuration interaction. Spin−orbit effects are included through the relativistic configuration interaction method. In contrast to HfCO, which exhibits a $^3\Sigma^-$ ground state, two nearly degenerate electronic states ($^5\Delta$, $^3\Sigma^-$) were found as candidates for the ground state of ZrCO. Both Hf and Zr form stable complexes with CO relative to the dissociation limits. The nature of bonding is discussed in terms of the wave function composition and the Mulliken population analysis.

1. Introduction

Zirconium and hafnium have been employed as catalysts for many years. They have also been used in transition-metal alloys with useful properties.[1−2] The synthesis, structure, and properties of zirconium and hafnium complexes and their reaction with carbon monoxide have also been studied extensively.[3−15] In particular, zirconium catalysts in carbon monoxide reactions have attracted considerable attention from a variety of standpoints such as oxidation,[16] hydrogenation,[17] and molecule activation.[18] In turn, carbon monoxide thermal desorption has been used to discuss the effect of zirconium diatomic molecules deposited on the crystal surface.[19] The influence of modifying additives of zirconium and cesium oxides on the state of transition metals has been studied by IR spectroscopy using adsorbed probe molecules such as carbon monoxide.[20]

To determine the spectroscopic properties, zirconium diatomic molecules such as ZrCo and Zr_2 were studied using a variety of spectroscopic techniques.[21,22] Small molecules of hafnium such as HfH has been discussed by our group,[23] and clusters such as Zr_3, Zr_4, and Zr_5 have been studied by our laboratory.[24−26] To gain insight into the nature of the interaction of Zr and Hf atoms with CO and to shed light on the low-lying electronic states of these species, we undertake a systematic comparative study of ZrCO and HfCO. We employ a complete active space multiconfiguration self-consistent field (CASMCSCF) technique to determine the potential curves and their corresponding electronic configurations. Subsequently, multireference singles + doubles configuration interaction (MRSDCI) was used to determine the equilibrium geometries, minimum energies, and dissociation energies for the low-lying states. Mulliken populations and vibrational frequencies were computed from the wave functions. Relativistic configuration interaction (RCI) calculations were considered to discuss the importance of the spin−orbit coupling effects for the HfCO complex.

2. Method of Calculations

Relativistic effective core potentials (RECPs) taken from the work of Ross et al.,[27] which retained the outer $4s^24p^64d^25s^2$ shells of the Zr atom and the $5s^25p^65d^26s^2$ shells of the Hf atom in the valence space, were employed in this study. For the carbon and oxygen atoms, the RECPs taken from Pacios and Christiansen, which retained the outer $2s^22p^2$ and $2s^22p^4$ shells, respectively, were employed.[28] The optimized valence (5s5p4d) Gaussian basis sets for the Zr and Hf atoms were taken from ref 27. The (4s4p) optimized Gaussian basis sets for the carbon and oxygen atoms from ref 28 were contracted to (3s3p). The carbon and oxygen basis sets were supplemented with one set of 3d functions generated from Dunning and Hay,[29] with $\alpha_d = 0.75$ for carbon and $\alpha_d = 0.85$ for oxygen, respectively. The effect of 4f-type functions was found to be very small, especially at the MRSDCI level, on the geometries and energy separations for transition-metal-containing species, as demonstrated by our earlier studies.[38] Furthermore, comparison of energy separations at the dissociation limit with the experimental atomic energy separations of the transition-metal atoms demonstrate that the basis sets and the correlation techniques used are quite adequate for the computation of potential energy surfaces.

The ZrCO and HfCO species were computed in the C_{2v} point group with the *z*-axis chosen as the C_2-axis. The orientation is relevant to describe the orbitals and the active space. According to the low-lying spectral terms of the zirconium and hafnium atoms,[30] we calculated the first root at the CASMCSCF level for each electronic state of all possible spin multiplicities and different bond lengths varying from 1.4 to 8.0 Å. Let n_i represent the number of inactive orbitals and n_a be the active orbitals of four irreducible representations under the C_{2v} group. At infinite separation between all atoms, the $(n-1)$s, $(n-1)$p, $(n-1)$d, and *n*s atomic orbitals of zirconium ($n = 5$) or hafnium ($n = 6$) and the 2s, 2p atomic orbitals of the carbon and oxygen span 10 a_1, 4 b_1, 4 b_2, and 1 a_2 orbital in the C_{2v} group. Among these, the semicore $(n-1)$s and $(n-1)$p orbitals of zirconium or hafnium and 2s, $2p_y$, and $2p_x$ of oxygen were found to be unimportant for the interaction of Zr(Hf) and CO. These orbitals comprise three a_1, two b_1, and two b_2, which

[†] Arizona State University.
[‡] Tsinghua University.

S1089-5639(97)02897-1 CCC: $15.00
Published on Web 02/05/1998

TABLE 1: Reference Configurations for the RCI Calculations of Hf−CO with Spin−Orbit Interactions

configurations						$\omega-\omega$ state				
1σ	2σ	3σ	1π	1δ	$\lambda-$s state	0^+	0^-	1	2	3
2	2	2	2	0	$^3\Sigma^-$	4		2		
2	2	2	2	0	$^1\Delta$				4	
2	2	1	2	1	$^5\Delta$	24	24	24	24	24
2	2	2	1	1	$^3\Pi$	8	8	8	8	8
total reference configurations						36	32	34	36	32
total determinants						18 404	17 644	18 036	18 404	17 672

TABLE 2: Atomic Energy Separations of Zr + CO Obtained from the Asymptotic Molecular Energy Separations at the Dissociation Limit[a]

molecular states	dissociation limit	CASMCSCF (cm^{-1})	MRSDCI (cm^{-1})	exptl (cm^{-1})
$^3\Sigma^-$, $^3\Pi$, $^3\Delta$	$(4d^25s^2)a^3F + {}^1\Sigma^+$	0	0	0
$^1\prod$, $^1\Delta$	$(4d^25s^2)a^1D + {}^1\Sigma^+$	7317	5518 (5504)	5102
$^5\Pi$, $^5\Delta$	$(4d^35s)a^5F + {}^1\Sigma^+$	6556	5553 (6529)	5460

[a] The distance between Zr and C is 8.00 Å. The values in parentheses included the Davison correction.

TABLE 3: Atomic Energy Separations of Hf + CO Obtained from the Asymptotic Molecular Energy Separations at the Dissociation Limit[a]

molecular state	dissociation limit	CASMCSCF (cm^{-1})	MRSDCI (cm^{-1})	exptl (cm^{-1})
$^3\Sigma^-$, $^3\Pi$, $^3\Delta$	$(5d^26s^2)a^3F + {}^1\Sigma^+$	0	0	0
$^1\Pi$, $^1\Delta$	$(5d^26s^2)a^1G + {}^1\Sigma^+$	5952	5513 (4978)	7790
$^5\Phi$, $^5\Delta$	$(5d^36s)a^5F + {}^1\Sigma^+$	11575	15163 (15611)	13643

[a] The distance between Hf and C is 8.00 Å. The values in parentheses included the Davison correction.

were kept inactive, while the others were included in the active space. The CASMCSCF computations for both ZrCO and HfCO included excitations of eight electrons in all possible ways among seven a_1, two b_2, two b_1 and one a_2 orbital in the active space, while excitations from the inactive orbitals were not allowed at the CASMCSCF level of calculations although these orbitals were allowed to relax. This choice yields $n_i = 3, 2, 2, 0$ (a_1, b_2, b_1, a_2) and $n_a = 7, 2, 2, 1$. However, the choice $n_a = 7, 2, 2, 1$ leads to too large a number of configurations, and thus we kept the lowest a_1 orbital inactive, which resulted in $n_a = 6, 2, 2, 1$. This selection generates the correct dissociation limit for both Zr + CO and Hf + CO systems.

The MRSDCI calculations were carried out for the low-lying states, in which single and double excitations were allowed. Reference configurations with coefficients ≥ 0.05 were chosen from the CASMCSCF computations and included in the MRSDCI calculations. The CASMCSCF calculation included up to 12 740 configuration spin functions (CSFs), while the MRSDCI included up to 450 173 CSFs.

The spin−orbit effects were introduced through the relativistic configuration interaction (RCI) scheme developed by one of the authors.[31] In this scheme all low-lying $\lambda-$s states that give rise to the same Ω state were mixed in a multireference singles and doubles CI including spin−orbit coupling. Table 1 shows a list of reference configurations that were included in the RCI for the various Ω states. Consider $\Omega = 0^+$ as an example; this state contained 4 reference configurations from $1\sigma^22\sigma^23\sigma^21\pi^2$, 24 reference configurations from $1\sigma^22\sigma^23\sigma^11\pi^21\delta^1$, and 8 reference configurations from $1\sigma^22\sigma^23\sigma^21\pi^21\delta^1$. Single and double excitations from these reference configurations generated 18 404 determinants. The spin−orbit integrals derived from the RECPs using Pitzer's Argos codes[32] were transformed in the MRSDCI natural orbitals obtained in the absence of spin−orbit coupling. These integrals were then added to the CI Hamiltonian matrix in the RCI. All of the CASMCSCF/CI calculations were made by using one of the author's modified version of ALCHEMY II codes[33] to include RECPs.[34]

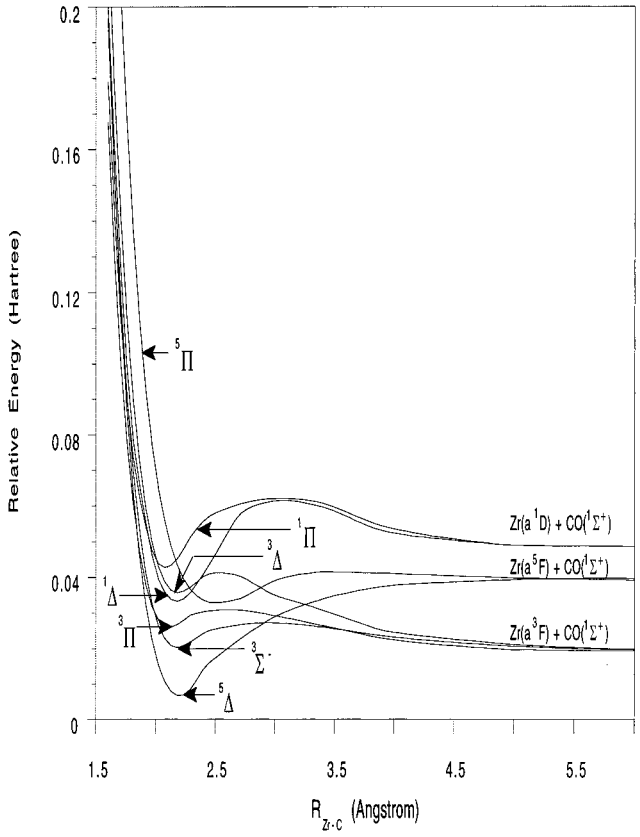

Figure 1. Potential energy curves of ZrCO as a function of the Zr−C distance in its different low-lying electronic states.

3. Results and Discussion

A. Atomic Energy Separations of Zr and Hf. Tables 2 and 3 show the possible molecular electronic states of ZrCO and HfCO generated from their respective atomic states. We set the distance between the transition-metal atom (Zr or Hf) and CO to 8.00 Å to obtain the energy separations at the dissociation limit. As seen from Table 2, the ground state of Zr is computed as the a^3F state arising from the $4d^25s^2$ configuration, which is in agreement with the experimental atomic spectra from ref 30. Singlet states converged to the $(4d^25s^2)a^1D + CO(^1\Sigma^+)$ dissociation limit. We have calculated the relative energy with respect to the lowest $(4d^25s^2)a^3F + CO(^1\Sigma^+)$ dissociation limit as 7317 and 5518 cm^{-1} at the CASMCSCF and MRSDCI levels, respectively. The MRSDCI value is in good agreement with the experimental data of 5102 cm^{-1}. Quintet states converged to the $(4d^35s)a^5F + CO(^1\Sigma^+)$ dissociation limit. The relative energy with respect to the same atomic ground state was 6556 and 5553 cm^{-1} at the CASMC-

TABLE 4: Spectroscopic Properties and Energy Separations of the Electronic States of ZrCO[a]

	CASMCSCF					MRSDCI				
state	Zr−C (Å)	C−O (Å)	T_e (cm^{-1})	ω_e (cm^{-1})	D_e (eV)	Zr−C (Å)	C−O (Å)	T_e (cm^{-1})	ω_e (cm^{-1})	D_e (eV)
$^5\Delta$	2.222	1.149	0	2132	0.169	2.193	1.155	0	2143	0.414
$^3\Sigma^-$	2.194	1.143	3825	2129	−0.305	2.173	1.146	189 (−959)	2133	0.391
$^3\Pi$	2.113	1.167	4749	2169	−0.420	2.104	1.169	3070 (2682)	2163	0.033
$^1\Delta$	2.184	1.152	6613	2142	−0.651	2.168	1.154	3073 (2087)	2138	0.033
$^3\Delta$	2.195	1.154	7100	2119	−0.711	2.183	1.158	5331 (4486)	2140	−0.247
$^1\Pi$	2.094	1.175	8230	2057	−0.851	2.087	1.178	5671 (5096)	2057	−0.289
$^5\Pi$	2.510	1.132	6641	2087	−0.654	2.411	1.136	7859 (8186)	2098	−0.560

[a] ω_e stands for the vibrational frequency of the C−O bond. The values in parentheses include the Davidson correction.

SCF and MRSDCI levels, respectively. Again the MRSDCI result is in excellent agreement with 5460 cm^{-1} derived from the atomic spectra.[30] The CASMCSCF calculations show that the singlet states at the dissociation limit are higher than the quintet states, while the MRSDCI calculations, which are more accurate, place them closer to the experimental data. The gross Mulliken populations of zirconium for the triplet, singlet, and quintet states at the dissociation limit were calculated as $4d^{1.99}5s^{1.85}$, $4d^{2.08}5s^{1.77}$, and $4d^{2.99}5s^{1.00}$, respectively, which show that the assignments for the different dissociation limits are consistent with the experimental data.

As seen from Table 3, the ground state of Hf at the dissociation limit is computed as the a^3F state arising from the $5d^26s^2$ configuration, in agreement with the experimental atomic spectral data from ref 30. The singlet states converged to the $(5d^26s^2)a^1G + CO(^1\Sigma^+)$ dissociation limit. We have calculated the relative energy with respect to the $(5d^26s^2)a^3F + CO(^1\Sigma^+)$ dissociation limit as 5952 and 5513 cm^{-1} at the CASMCSCF and MRSDCI levels, respectively, which reasonably agree with the experimental value of 7790 cm^{-1}. Quintet states converged to the dissociation limit generated from $(5d^36s)a^5F + CO(^1\Sigma^+)$. The relative energy with respect to the $(5d^26s^2)a^3F + CO(^1\Sigma^+)$ dissociation limit was computed as 11 575 and 15 163 cm^{-1} at the CASMCSCF and MRSDCI levels, respectively. These results are also in agreement with experimentally derived value of 13 643 cm^{-1}. The gross Mulliken populations of hafnium for the triplet, singlet, and quintet states at the dissociation limit were calculated as $5d^{1.99}6s^{1.85}$, $5d^{1.91}6s^{1.91}$, and $5d^{2.97}6s^{1.00}$, respectively, which are consistent with the experimental data. The computed atomic energies at the dissociation limit provide confidence in our computed values. Our computed R_e and ω_e values of the free diatomic CO obtained from MRSDCI are 1.140 Å and 2156 cm^{-1} compared to experimental values[35] of 1.128 Å and 2170 cm^{-1}, respectively.

B. Potential Energy Curves and Equilibrium Properties of ZrCO. As discussed in ref 36, the M−OC complex, where M stands for a transition metal, is found to be repulsive, and thus only the M−CO orientation was studied. Figure 1 shows the CASMCSCF potential energy curves of the low-lying states of ZrCO. As can be seen from Figure 1, the CASMCSCF curves differ from the experimental atomic states for the quintet and singlet states at the dissociation limit, but the MRSDCI calculations gave the correct sequences, although quintet and singlet states at the dissociation limit are very close to each other. Thus the CASMCSCF results give qualitative accuracies, while more quantitative results are obtained at a more accurate MRSDCI level.

Table 4 shows the equilibrium geometries, spectroscopic properties, and the energy separations of the electronic states of ZrCO at both CASMCSCF and MRSDCI levels. As seen from Table 4 and Figure 1, the ground state of ZrCO is $^5\Delta$, but the lowest excited state, $^3\Sigma^-$, is very close to $^5\Delta$. We compute the relative energy of $^3\Sigma^-$ with respect to $^5\Delta$ as 3825 cm^{-1} at the CASMCSCF level. More accurate MRSDCI calculations, however, lower the energy separation to only 189 cm^{-1}, while the quadruple cluster correction reverses the relative order. This suggests that both $^5\Delta$ and $^3\Sigma^-$ states are candidates for the ground state of ZrCO. The equilibrium distances of Zr−C and C−O for the $^5\Delta$ state are 2.222 and 1.149 Å at the CASMCSCF level, while they become 2.193 and 1.155 Å at the MRSDCI level. Higher order correlation effects included in the MRSDCI seem to generally shrink the Zr−C bond. As expected, the R_e of Zr−C of the $^5\Delta$ state shrinks by 0.03 Å at the MRSDCI level compared to the CASMCSCF results. The R_e of the C−O bond remains almost the same in the formation of the ZrCO complex. As to the $^3\Sigma^-$ state, the equilibrium distances of Zr−C and C−O are 2.194 and 1.143 Å at the CASMCSCF level, and 2.173 and 1.146 Å, respectively, at the MRSDCI level. High-order CI calculations shrink the Zr−C bond length by 0.02 Å.

Our computed CO vibrational frequency values for most of the states are around 2050−2170 cm^{-1}. This shows about 9% reduction of the CO vibrational frequency in ZrCO with respect to the free CO vibrational frequency of 2260 cm^{-1} at the MRSDCI level. The lowest lying states were calculated as $^3\Pi$, $^1\Delta$, and $^3\Delta$, etc.

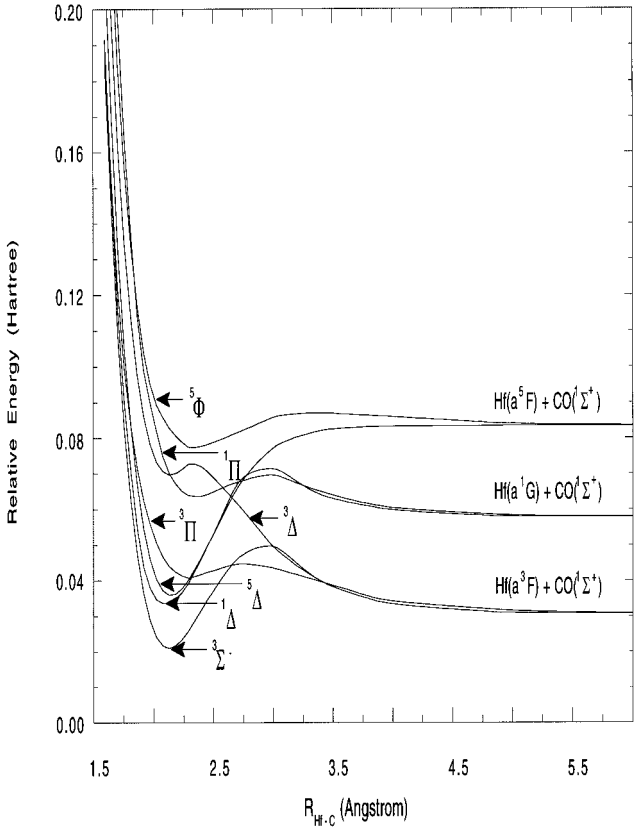

Figure 2. Potential energy curves of HfCO as a function of the Hf−C distance in its different low-lying electronic states.

TABLE 5: Spectroscopic Properties and Energy Separations of the Electronic States of HfCO[a]

	CASMCSCF						MRSDCI				
state	Hf−C (Å)	C−O (Å)	Hf−O (Å)	T_e (cm^{-1})	ω_e (cm^{-1})	D_e (eV)	Hf−C (Å)	C−O (Å)	T_e (cm^{-1})	ω_e (cm^{-1})	D_e (eV)
$^3\Sigma^-$	2.134	1.153	3.287	0	2149	0.276	2.126	1.156	0 (0)	2153	0.922 (1.12)
$^1\Delta$	2.138	1.160	3.298	2794	2154	−0.070	2.134	1.161	3042 (3362)	2154	0.545 (0.705)
$^5\Delta$	2.149	1.158	3.307	3198	2146	−0.121	2.134	1.163	7756 (9001)	2156	−0.039 (0.007)
$^3\Pi$	2.307	1.136	3.443	4394	2094	−0.269	2.288	1.143	5546 (6850)	2109	0.235 (0.273)

[a] ω_e stands for the vibrational frequency of the C−O bond. The values in parentheses include the Davidson correction.

TABLE 6: Spectroscopic Constants of the Low-Lying States of Hf−CO Including the Spin−Orbit Effects

			Hf−C (Å)		C−O (Å)		T_e, cm^{-1}		ω_e, cm^{-1}	
$\omega-\omega$ state	main composition		SO	NO SO	SO	NO SO	SO	NO SO	SO	NO SO
0^+	92% $^3\Sigma^-$	6% $^5\Delta$	2.132	2.126	1.156	1.156	−294	0	2153	2153
1	91% $^3\Sigma^-$	6% $^5\Delta$	2.128	2.126	1.156	1.156	−103	0	2153	2153
2	88% $^1\Delta$	8% $^5\Delta$	2.136	2.134	1.160	1.161	2891	3042	2152	2154
0^-	97% $^5\Delta$		2.137	2.134	1.162	1.163	7385	7756	2155	2156
3	97% $^5\Delta$		2.136	2.134	1.163	1.163	7501	7756	2157	2156
1 (II)	97% $^5\Delta$		2.138	2.134	1.163	1.163	7504	7756	2155	2156

The dissociation energies (D_e) of the $^5\Delta$ state of ZrCO with respect to the Zr(a^{3}F)+CO($^1\Sigma^+$) dissociation limit were computed as 0.169, 0.414, and 0.467 eV at the CASMCSCF, MRSDCI, and MRSDCI+Q levels, respectively. The D_e of $^3\Sigma^-$, another candidate for the ground state of ZrCO, was computed with respect to the same dissociation limit as 0.391 and 0.586 eV at the MRSDCI and MRSDCI+Q levels, respectively.

C. Potential Energy Curves and Equilibrium Properties of HfCO without Spin−Orbit Coupling. Figure 2 shows the CASMCSCF potential energy curves of the low-lying states of HfCO, while Table 5 shows the equilibrium geometries, spectroscopic properties, and energy separations of bound electronic states of HfCO at both CASMCSCF and MRSDCI levels. As seen from Table 5 and Figure 2, unlike ZrCO, the ground state of HfCO is unambiguously $^3\Sigma^-$. The equilibrium Hf−C and C−O distances are 2.134 and 1.153 Å at CASMCSCF level, and 2.126 and 1.156 Å at the MRSDCI level, respectively. As expected, the R_e of Hf−C of the $^3\Sigma^-$ state shrinks at the MRSDCI level by about 0.01 Å compared to the CASMCSCF results, while the R_e of the C−O bond remains almost unchanged, suggesting that the bond strength of CO is little changed in the formation of the HfCO complex.

Our computed CO vibrational frequency values for most of the states are around 2100−2160 cm^{-1}, yielding a 6% reduction in the CO vibrational frequency in HfCO with respect to the free CO vibrational frequency of 2260 cm^{-1} at the MRSDCI level. The excited states were calculated as $^1\Delta$, $^5\Delta$, and $^3\Pi$, etc., among which the $^1\Delta$ and $^5\Delta$ states were found to be the lowest. Consider $^1\Delta$ as an example, its relative energy with respect to the $^3\Sigma^-$ ground state near the equilibrium geometry is 2794 and 3042 cm^{-1} at the CASMCSCF and MRSDCI levels, respectively.

The D_e values of the $^3\Sigma^-$ state for HfCO relative to the Hf(a^{3}F)+CO($^1\Sigma^+$) dissociation limit was computed as 0.276, 0.922, and 1.12 eV at the CASMCSCF, MRSDCI, and MRSDCI+Q levels, respectively. This shows that the D_e value is strongly influenced by higher order electron correlation effects.

D. Spin−Orbit Effects for HfCO. Table 6 shows the effect of spin−orbit (SO) coupling on the low-lying electronic states of HfCO near their equilibrium geometries. The states are designated with their Ω quantum numbers. The ground state is found to be the 0^+ state with Hf−C = 2.132 and C−O = 1.156 Å when the spin−orbit coupling is included, compared to Hf−C = 2.126 and C−O = 1.156 Å without spin−orbit correction. Thus the R_e values of the ground state are not affected much by the spin−orbit effect as the leading configuration of 0^+ is dominated by $^3\Sigma^-$. The energy separations (T_e) do not change too much by SO coupling. For example, the 0^+-1 energy separation is 191 cm^{-1}.

TABLE 7: Leading Configurations in the MRSDCI Wave Functions of the Low-Lying Electronic States of Zr−CO and Hf−CO[a]

	weights (%)		configurations					
state	ZrCO	HfCO	2σ	3σ	4σ	1π	2π	1δ
$^3\Sigma^-$	81	86	2	2	0	2	0	0
	5		2	0	0	2	0	2
$^5\Delta$	92	92	2	1	0	2	0	1
$^1\Delta$	71	83	2	2	0	2	0	0
	5		2	1	0	2	0	1
		3	2	2	0	0	2	0
$^3\Pi$	85		2	1	0	3	0	0
		83	2	2	0	1	0	1
		3	2	0	0	3	0	1
$^3\Delta$	89	91	2	1	0	2	0	1
$^1\Pi$	86		2	1	0	3	0	0
		64	2	2	1	1	0	0
		26	2	2	0	1	0	1
$^5\Pi$	97		2	1	0	1	0	2
$^5\Phi$		98	2	1	1	1	0	1

[a] $4s^24p^6$ shells of Zr atom and $5s^25p^6$ shells of Hf atom are included.

E. The Nature of the Low-Lying Electronic States. Table 7 shows the leading configurations in the MRSDCI wave functions of low-lying electronic states of ZrCO and HfCO. For HfCO the 1σ, 2σ, 3σ, 4σ, 1π, and 2π orbitals were found to be strongly bonding. These orbitals were mainly composed of

$$\psi[1\sigma] = -\mathrm{O(p)} - \mathrm{C(s)} + \mathrm{C(p)}$$

$$\psi[2\sigma] = \mathrm{C(s)} + \mathrm{C(p)} + \mathrm{Hf(s)} + \mathrm{Hf(p)}$$

$$\psi[3\sigma] = \mathrm{Hf(s)} + \mathrm{Hf}(d_{x^2+y^2-2z^2})$$

$$\psi[4\sigma] = \mathrm{O(s)} + \mathrm{C(s)} + \mathrm{C(p)} - \mathrm{Hf(s)} + \mathrm{Hf(p)} - \mathrm{Hf}(d_{x^2+y^2-2z^2})$$

$$\psi[1\pi] = \begin{cases} -\mathrm{O}(p_x) + \mathrm{C}(p_x) - \mathrm{Hf}(d_{xz}) \\ -\mathrm{O}(p_y) + \mathrm{C}(p_y) - \mathrm{Hf}(d_{yz}) \end{cases}$$

$$\psi[2\pi] = \begin{cases} \mathrm{C}(p_x) + \mathrm{Hf}(p_x) + \mathrm{Hf}(d_{xz}) \\ \mathrm{C}(p_y) + \mathrm{Hf}(p_y) + \mathrm{Hf}(d_{yz}) \end{cases}$$

TABLE 8: Mulliken Population Analysis for the Low-Lying Electronic States of ZrCO and HfCO

		gross population									
species	state	O	C	M	O (s)	O (p)	C (s)	C (p)	M (s)	M (p)	M (d)
ZrCO	$^5\Delta$	6.512	3.962	11.53	1.936	4.530	1.568	2.306	2.832	6.079	2.616
	$^3\Sigma^-$	6.488	3.868	11.64	1.934	4.507	1.530	2.251	3.453	6.103	2.087
	$^3\Pi$	6.542	4.011	11.45	1.932	4.565	1.541	2.379	2.801	6.100	2.546
	$^1\Delta$	6.495	3.945	11.56	1.938	4.512	1.530	2.329	3.293	6.126	2.141
	$^3\Delta$	6.513	4.029	11.46	1.940	4.527	1.564	2.378	2.768	6.185	2.505
	$^1\Pi$	6.544	4.012	11.44	1.932	4.567	1.523	2.397	2.802	6.139	2.503
HfCO	$^3\Sigma^-$	6.541	3.839	11.62	1.953	4.543	1.416	2.334	3.695	6.197	1.727
	$^5\Delta$	6.560	3.922	11.52	1.949	4.565	1.463	2.370	3.033	6.107	2.379
	$^1\Delta$	6.540	3.902	11.56	1.953	4.541	1.422	2.392	3.727	6.172	1.659
	$^3\Pi$	6.497	3.847	11.66	1.965	4.485	1.450	2.314	3.701	6.250	1.704

As seen from Table 7, the $^5\Delta$ state of ZrCO is predominantly composed of $1\sigma^2 2\sigma^2 3\sigma^1 1\pi^2 1\delta^1$ with a coefficient ≥ 0.92, while the $^3\Sigma^-$ state is predominantly composed of $1\sigma^2 2\sigma^2 3\sigma^1 1\pi^2 1\delta^1$ with a coefficient ≥ 0.81. The excited states are usually based on the excitation of an electron from an occupied orbital to unoccupied one. For HfCO, the $^3\Sigma^-$ state is predominantly composed of $1\sigma^2 2\sigma^2 3\sigma^2 1\pi^2$ with a coefficient ≥ 0.86.

The Mulliken populations of the low-lying states of ZrCO and HfCO are presented in Table 8. The standard description of bonding of metal carbonyls is one of donation from the highest occupied σ orbital (which is essentially a carbon lone pair) to the metal atom followed by a π back-donation from the metal atom to the carbonyl π^* antibonding orbital with a large carbon component. As seen from Table 8, the $^5\Delta$ state of ZrCO is composed of Zr($s^{2.832}p^{6.079}d^{2.616}$), C($2s^{1.568}2p^{2.306}$), and O($2s^{1.936}2p^{4.530}$) populations. The free Zr and CO populations obtained from the Zr(a^5F) + CO($^1\Sigma^+$) dissociation limit are Zr($s^{2.998}$ $p^{6.010}d^{2.993}$), C($2s^{1.754}2p^{1.828}$), and O($2s^{1.821}2p^{4.463}$). Thus, in the formation of $^5\Delta$, there is a primary transfer of electron density from the carbon 2s orbital (0.19*e*) to the zirconium. Zirconium (dπ) in turn donates about 0.37*e* charge to the pπ orbital of CO, while the 6s orbital loses 0.17*e* alongside the C_2-axis. Consequently, the net population of zirconium has decreased by about 0.47*e*, while carbon and oxygen populations increase by 0.29 and 0.18*e*, respectively. This implies that the dπ−pπ type of bonding plays an important role.

Another possible candidate for the ground state of ZrCO, $^3\Sigma^-$, is composed of Zr($s^{3.453}p^{6.103}d^{2.087}$), C($2s^{1.530}2p^{2.251}$), and O($2s^{1.934}2p^{4.507}$), compared to the populations of Zr($s^{3.843}p^{6.162}d^{1.996}$), C($2s^{1.756}2p^{1.830}$), and O($2s^{1.821}2p^{4.460}$) obtained from the Zr($a^3F$) + CO($^1\Sigma^+$) dissociation limit. Consequently, there is primary transfer of electron density from the carbon 2s orbital (0.23*e*) to the zirconium in the formation of the ZrCO complex. In turn, the 6s orbital of zirconium loses about 0.39*e* charge, while the $2p_z$ orbital of carbon receives 0.42*e* charge. The 6p and 5d orbitals of zirconium remain almost unchanged, suggesting that the σ bonding plays an important role.

For the HfCO complex, relativistic mass−velocity effects[37] results in contraction and stabilization of the 6s orbital of the Hf atom. Consequently, the 6s orbital can more readily accept the electronic charge from the carbon atom followed by back-donation of electronic charge from hafnium (dπ) to the π^* antibonding orbital of CO. As seen from Table 8, the $^3\Sigma^-$ state of HfCO is composed of Hf($s^{3.695}p^{6.197}d^{1.727}$), C($2s^{1.416}2p^{2.334}$), and O($2s^{1.953}2p^{4.543}$). The free Hf and CO populations obtained from the Hf(a^3F) + CO($^1\Sigma^+$) dissociation limit are Hf($s^{3.860}p^{6.151}d^{1.989}$), C($2s^{1.755}2p^{1.829}$), and O($2s^{1.821}2p^{4.463}$). Thus, in the HfCO bond formation, there is a primary transfer of electron density from the carbon 2s orbital (0.34*e*) to the hafnium. Hafnium (dπ) in turn donates about 0.26*e* charge to the pπ orbital of CO. Consequently, the net population of hafnium decreases by 0.38*e*, while carbon and oxygen populations increase by 0.17 and 0.22*e*, respectively. This feature of the Mulliken population suggests that the electron transfer from CO is like a lone-pair transfer from carbon to the metal resulting in a σ bond, while the electronic charge transfer from the metal is the dπ−pπ bonding type. The populations of the s and p orbitals for oxygen are about the same, but for carbon and zirconium there is a greater change according to the states.

4. Conclusion

We obtained the potential energy curves and spectroscopic properties of the low-lying states for ZrCO and HfCO arising from three dissociation limits, namely, Zr(a^3F) + CO($^1\Sigma^+$), Zr(a^1D) + CO($^1\Sigma^+$), and Zr(a^5F) + CO($^1\Sigma^+$), Hf(a^3F) + CO($^1\Sigma^+$), Hf(a^1G) + CO($^1\Sigma^+$), and Hf(a^5F) + CO($^1\Sigma^+$), respectively. Two nearly degenerate electronic states, namely, $^5\Delta$ and $^3\Sigma^-$, were found as candidates for the ground state of ZrCO. The equilibrium bond lengths for the $^5\Delta$ and $^3\Sigma^-$ states are Zr−C = 2.193, C−O = 1.155 Å and Zr−C = 2.173, C−O=1.146 Å, respectively, at the MRSDCI level. The $^3\Sigma^-$ was found to be the ground state of the HfCO complex with an equilibrium geometry of Hf−C = 2.126 and C−O = 1.156 Å at the MRSDCI level without spin−orbit coupling. The ground state of HfCO including spin−orbit effects was found to be a 0^+ state. The dissociation energy values for all the low-lying states have been calculated. The nature of the low-lying electronic states is discussed through the CI coefficients and the Mulliken populations.

Acknowledgment. This research was supported by the U.S. Department of Energy under Grant No. DEFG02-86ER13558.

References and Notes

(1) Hughbanks, T.; Wang, C. C. *Inorg. Chem.* **1996**, *35*, 6987.
(2) Castellanos, M.; Martinez Chavez, M.; West, A. R. *Z. Kristallogr.* **1990**, *190*, 161.
(3) Jacoby, D.; Floriani, C.; Chiesi-Villa, A. *J. Am. Chem. Soc.* **1993**, *115*, 7025.
(4) Curtis, C. J.; Haltiwanger, R. C. *Organometallics* **1991**, *10*, 3220.
(5) Guram, A. S.; Guo, Z. Y.; Jordan, R. F. *J. Am. Chem. Soc.* **1993**, *115*, 4902.
(6) Anderson, G.; Lin, M. *Organometallics* **1988**, *7*, 2285.
(7) Erker, G.; Brackemeyer, T.; Frohlich, R. *Organometallics* **1997**, *16*, 531.
(8) Fryzuk, M. D.; Mylvaganam, M.; MacGillivary, L. R. *Organometallics* **1996**, *15*, 1134.
(9) Veith, M.; Mathur, S.; Huch, V. *J. Chem. Soc., Dalton Trans.* **1997**, *12*, 2101.
(10) Willey, G. R.; Butcher, M. L.; Drew, M. G. B. *J. Chem. Soc., Dalton Trans.* **1994**, *22*, 3285.
(11) Diamond, M. G.; Green, L. H. M.; Popham, A. N. *J. Chem. Soc., Dalton Trans.* **1993**, *16*, 2535.
(12) Braunstein, P.; Cauzzi, D.; Kelly, D. *Inorg. Chem.* **1993**, *32*, 3373.
(13) Corazza, F.; Solari, E.; Floriani, C. *J. Chem. Soc., Dalton Trans.* **1990**, *4*, 1335.

(14) Ellis, J. E.; Frerichs, S. R.; Stein, B. K. *Organometallics* **1993**, *12*, 1048.
(15) Waldman, T. E.; Stahl, L.; Wilson, D. R.*Organometallics* **1993**, *12*, 1543.
(16) Baiker, A.; Maciejewski, M.; Hug, P. *J. Catal.* **1995**, *151*, 407.
(17) Ishihara, T.; Iwakuni, H.; Eguchi, K. *Appl. Catal.* **1991**, *75*, 225.
(18) Silver, R. G.; Hou C. J.; Ekerdt, J. G. *J. Catal.* **1989**, *118*, 400.
(19) Bardi, U.; Ross, P. N. *Langmuir* **1993**, *9*, 132.
(20) Pestryakov, A. N.; Davydov, A. A. *Kinet. Catal.* **1996**, *37*, 859.
(21) Arrington, C. A.; Morse, M. D.; Doverstal, M. *J. Chem. Phys.* **1995**, *102*, 1895.
(22) Arrington, C. A.; Blume, T.; Morse, M. D. *J. Phys. Chem*. **1994**, *98*, 1398.
(23) Das, K. K.; Balasubramanian, K. *J. Mol. Spectrosc.* **1991**, *145*, 142.
(24) Majumdar, D.; Balasubramanian, K. Submitted for publication in *Chem. Phys. Lett*.
(25) Dai, D.; Balasubramanian, K. *Chem. Phys. Lett.* **1994**, *231*, 352.
(26) Dai, D.; Balasubramanian, K. *Chem. Phys. Lett.* **1992**,*193*, 565.
(27) LaJohn, L. A.; Christiansen, P. A.; Ross, R. B.; Atashroo, T.; Ermler, W. C. *J. Chem. Phys.* **1987**, *87*, 2812. Ross, R. B.; Powers, J. M.; Atashroo, T.; Ermler, W.; Lajohn, L. A.; Christiansen, P. A. *J. Chem. Phys*. **1990**, *93*, 6654.
(28) Pacios, L. F.; Christiansen, P. A. *J. Chem. Phys.* **1985**, *82*, 2664.
(29) Dunning, Jr. T. H.; Hay, P. J. In *Methods of Electronic Structure Theory*; Schaefer, H. F., III., Ed.; Plenum Press: New York, 1977; p 1.
(30) Moore, C. E. *Tables of Atomic Energy Levels*; National Bureau of Standards: Washington, DC, 1971.
(31) Balasubramanian, K. *J. Chem. Phys.* **1988**, *89*, 5731.
(32) Pitzer, R. M.; Winter, N. W. *J. Chem. Phys.* **1988**, *92*, 3061.
(33) The major authors of ALCHEMY II are B. Lengsfield, B. Liu, and Y. Yoshmine.
(34) Balasubramanian, K. *Chem. Phys. Lett.* **1986**, *127*, 585.
(35) Huber, K. P.; Herzberg, G. *Molecular Spectra and Molecular Structure IV, Constants of Diatomic Molecules*; Van Nostrand Reinhold: New York, 1979.
(36) Dai, D.; Balasubramanian, K. *J. Chem. Phys.* **1994**, *101*, 2148.
(37) Balasubramanian, K. *Relativistic Effects in Chemistry: Part A & B*, Wiley-Interscience: New York, 1997.
(38) Dai, D.; Balasubramanian, K. *Chem. Phys. Lett.* **1995**, 238, 207.